

Multicentury Changes to the Global Climate and Carbon Cycle: Results from a Coupled Climate and Carbon Cycle Model

G. BALA, K. CALDEIRA, A. MIRIN, AND M. WICKETT

Atmospheric Science Division, Lawrence Livermore National Laboratory, Livermore, California

C. DELIRE

ISE-M, Université Montpellier II, Montpellier, France

(Manuscript received 22 March 2005, in final form 12 May 2005)

ABSTRACT

A coupled climate and carbon (CO₂) cycle model is used to investigate the global climate and carbon cycle changes out to the year 2300 that would occur if CO₂ emissions from all the currently estimated fossil fuel resources were released to the atmosphere. By the year 2300, the global climate warms by about 8 K and atmospheric CO₂ reaches 1423 ppmv. The warming is higher than anticipated because the sensitivity to radiative forcing increases as the simulation progresses. In this simulation, the rate of emissions peaks at over 30 Pg C yr⁻¹ early in the twenty-second century. Even at the year 2300, nearly 50% of cumulative emissions remain in the atmosphere. Both soils and living biomass are net carbon sinks throughout the simulation. Despite having relatively low climate sensitivity and strong carbon uptake by the land biosphere, these model projections suggest severe long-term consequences for global climate if all the fossil fuel carbon is ultimately released into the atmosphere.

1. Introduction

Anthropogenic emissions of CO₂ from fossil fuels and land-use change are expected to lead to significant climate change in the future (Houghton et al. 2001). Both climate change and elevated CO₂ impact land and ocean carbon uptake. Photosynthesis by land plants is expected to increase with increased atmospheric CO₂ content (the so-called CO₂ fertilization effect) when water and nutrients are available (Curtis 1996; Koch and Mooney 1996; Mooney et al. 1999; Owensby et al. 1999), leading to increased terrestrial carbon uptake. Increased global temperatures are expected to increase heterotrophic respiration rates (Lloyd and Taylor 1994), diminishing or even reversing the net CO₂ flux from the atmosphere to the land biosphere (Cox et al. 2000; Friedlingstein et al. 2001; Cramer et al. 2001; Joos et al. 2001). Global warming is expected to reduce uptake of carbon by oceans (Sarmiento and Le Quere

1996; Sarmiento et al. 1998), because CO₂ is less soluble in warmer water and increased stratification would inhibit downward transport of anthropogenic carbon.

Here, we use a three-dimensional coupled ocean–atmosphere climate–carbon cycle general circulation model to study the feedbacks between the physical climate system and the carbon cycle. Cox et al. (2000) and Friedlingstein et al. (2001) described the first such models that represented the three-dimensional dynamical response of earth's climate and carbon system to CO₂ emissions. Cox et al. (2000) showed a very large positive feedback between the carbon cycle and the climate whereas Friedlingstein et al. (2001) showed a much weaker feedback. A feedback analysis by Friedlingstein et al. (2003) indicated that the differences between the model results were due primarily to Southern Ocean circulation and land biosphere response to global warming. However, land response to climate change was the dominant difference between the two model simulations of the twenty-first century. In the HadCM3 model (Cox et al. 2000, 2004; Betts et al. 2004), the land biosphere became a net source of CO₂ to the atmosphere, partly due to the dieback of the huge Amazonian forest, whereas in the Institut Pierre-Simon

Corresponding author address: Dr. G. Bala, Atmospheric Science Division, Lawrence Livermore National Laboratory, Livermore, CA 94550.
E-mail: bala1@llnl.gov

Laplace (IPSL) model (Friedlingstein et al. 2001), the land biosphere remained a net sink of CO₂ from the atmosphere.

Zeng et al. (2004) performed a fully coupled carbon–climate simulation and several sensitivity runs for the period of 1860–2100 with prescribed Intergovernmental Panel on Climate Change (IPCC) Special Report on Emission Scenarios (SRES) A1B emission scenario. Their results also indicated a positive feedback to global warming from the interactive carbon cycle, with an additional increase of 90 ppmv in the atmospheric CO₂, and 0.6-K additional warming. However, the changes in various carbon pools were more modest, due largely to the multiple limiting factors constraining terrestrial productivity and carbon loss. They suggest that the large differences among the models are manifestations of some of the poorly constrained processes such as the global strength of the CO₂ fertilization effect and the turnover time and rates of soil decomposition.

Using an interactive climate and carbon cycle model, Govindasamy et al. (2005) studied the enhancement of the carbon cycle feedback with climate sensitivity to greenhouse gas radiative forcing (amount of global warming per doubling of atmospheric CO₂ concentrations). In that investigation, in the high climate sensitivity case, year 2100 global warming was 8 K and land carbon uptake was 29% of total CO₂ emissions; in the zero climate sensitivity case, there was little warming and land uptake was 47% of total emissions. The atmospheric CO₂ concentration increased 48% more in the run with 8-K global climate warming than in the case with no warming. These results indicated that carbon cycle amplification of climate warming would be greater if there were higher climate sensitivity to increased atmospheric CO₂ content.

Using the same model, Thompson et al. (2004) attempted to bracket the uncertainty in terrestrial uptake arising from uncertainty in the land–biosphere–CO₂ fertilization effect. They performed one simulation in which the land–biosphere model was very sensitive to CO₂ fertilization and another simulation in which the land uptake was restrained by limiting CO₂ fertilization at present-day levels. The fertilization-limited run was designed to represent the possibility that the CO₂ fertilization effect could saturate rapidly, perhaps because of nutrient limitations. Through year 2100, the land was a very strong sink of carbon in the CO₂-fertilized simulation, but it became a source of carbon to the atmosphere in the fertilization-limited simulation. The predicted atmospheric CO₂ at year 2100 differed by 336 ppmv between the two cases. In the fertilization-limited run, the vegetation biomass was stable, but the soil car-

bon pool was shrinking because of climate change–induced increases in heterotrophic respiration.

Mathews et al. (2005) investigated the climate–carbon feedbacks in the University of Victoria (Uvic) climate–carbon cycle model. Several results from their modeling study are complimentary to the results from the work by Govindasamy et al. (2005), notably the increase in carbon–climate feedback with climate sensitivity, and persistence of the terrestrial carbon sink over the twenty-first century. In their model, the positive feedback between the carbon cycle and climate was found to be relatively small, resulting in an increase in simulated CO₂ of 60 ppmv in the coupled simulation at the year 2100. Including non-CO₂ greenhouse gas forcing and increasing the model's climate sensitivity increases the effect of this feedback to 140 ppmv. Mathews et al. (2005) also suggest differences in the net primary productivity (NPP) response to climate changes and hence an additional contributor to the spread of feedbacks simulated by models.

Previous coupled modeling studies without the carbon cycle component have mostly investigated doubled-CO₂, quadrupled-CO₂, and other CO₂-stabilization scenarios. The recent coupled climate and carbon cycle models have focused on projections of climate change and the carbon cycle feedback over the twenty-first century (Cox et al. 2000; Friedlingstein et al. 2001; Govindasamy et al. 2005; Zeng et al. 2004). The recent modeling studies suggest that carbon cycle consequences of global warming are likely to amplify the effect of CO₂ emissions, because increased respiration rates at higher temperatures would induce carbon loss from the land biosphere to the atmosphere. These models have not been used previously to study the multi-century impact of large-scale fossil fuel emissions on climate and the carbon cycle out to the year 2300. Recent coupled modeling studies have suggested that the climate sensitivity to radiative forcing increases with time in long integrations (Senior and Mitchell 2000; Gregory et al. 2004), suggesting that warming in multi-century simulations will be larger than anticipated from the results of single-century simulations.

In this study, we address the global climate and carbon cycle changes out to the year 2300 that would occur if CO₂ emissions from all the currently estimated fossil fuel resources were released to the atmosphere. We use the coupled climate and carbon cycle model of Thompson et al. (2004). The major purpose is to investigate the time evolution of climate and its sensitivity to greenhouse gas radiative forcing, the time evolution of the carbon cycle feedback with climate, and the fate of emissions of all available fossil fuels in such a long simulation. Our simulations indicate that eventual at-

mospheric release of CO₂ from all fossil fuel resources could produce about 8-K warming of global and annual mean surface temperature by the year 2300. We note that our results are from a single modeling study, and validation using other coupled climate and carbon cycle models is required.

2. Model

To investigate the long-term impacts of climate change due to anthropogenic emissions, we use the Integrated Climate and Carbon (INCCA), the coupled climate and carbon cycle model (Thompson et al. 2004; Govindasamy et al. 2005). The physical ocean–atmosphere model is the National Center for Atmospheric Research (NCAR) Department of Energy (DOE) Parallel Climate Transitional Model (PCTM) model (Meehl et al. 2004; Washington et al. 2000), which is a version of the NCAR Community Climate Model (CCM) version 3.2 model (Kiehl et al. 1996) coupled to the Los Alamos National Laboratory (LANL) Parallel Ocean Program (POP) dynamic ocean model (Dukowicz and Smith 1994; Maltrud et al. 1998). The climate model is coupled to a terrestrial biosphere model, the Integrated Biosphere Simulator version 2 (IBIS2; Foley et al. 1996; Kucharik et al. 2000) and an ocean biogeochemistry model based on the Ocean Carbon cycle Model Intercomparison Project (OCMIP) biotic protocols (Thompson et al. 2004; Najjar and Orr 1999). The horizontal resolution of the land and atmosphere models is approximately 2.8° latitude × 2.8° longitude. The ocean model has a horizontal resolution of (2/3)°. The atmosphere and ocean models have 18 and 40 levels in the vertical, respectively.

Land surface biophysics, terrestrial carbon flux, and global vegetation dynamics are represented in a single, physically consistent modeling framework within IBIS2. IBIS2 simulates surface water, energy, and carbon fluxes on hourly time steps and integrates them over the year to estimate annual water and carbon balance. The annual carbon balance of vegetation is used to predict changes in the leaf area index and biomass for each of 12 plant functional types (8 types of trees, 2 types of shrubs, and 2 types of grasses), which compete for light and water using different ecological strategies. IBIS2 uses physiologically based formulations of photosynthesis (Farquhar et al. 1980; Collatz et al. 1992), stomatal conductance (Collatz et al. 1991), and respiration (Amthor 1984). IBIS2 also simulates carbon cycling through litter and soil organic matter. When driven by observed climatological datasets, the model's near-equilibrium runoff, NPP, and vegetation catego-

ries show a fair degree of agreement with observations (Foley et al. 1996; Kucharik et al. 2000).

The ocean biogeochemistry model is based on the OCMIP biotic protocols (Najjar and Orr 1999). This model predicts air–sea CO₂ fluxes; biogenic export of organic matter and calcium carbonate; and distributions of dissolved inorganic carbon, phosphate, oxygen, alkalinity, and dissolved organic matter. In the OCMIP protocol, export of biogenic materials is computed to maintain observed upper-ocean nutrient concentrations. However, because our simulations involve changes in ocean circulation, we cannot assume that surface nutrient concentrations remain stationary. Therefore, the OCMIP export formulation for biogenic materials is replaced with a formulation based on that of Maier-Reimer (1993).

The physical climate model PCTM does not use flux correction. However, when we coupled IBIS2 to PCTM, precipitation biases in the climate model led to vegetation distribution errors that, in turn, amplified the precipitation biases. This erroneous feedback resulted in unacceptable vegetation distribution in the control simulation, particularly in the Amazon. We applied a “precipitation correction” scheme that maintains global conservation of water and energy to remedy the errors in the vegetation distribution, as discussed in Govindasamy et al. (2005).

3. Experiments

We developed a year 1870 “preindustrial” initial condition with more than 200 yr of fully coupled equilibration before the start of experiments. During the first half of this spinup period, changes in soil carbon pools were accelerated by a factor of 40. Before this coupled spinup, the individual components PCTM, IBIS2, and the ocean biogeochemistry had been individually spun up. We perform two model simulations starting from the preindustrial initial conditions: a “control” case with no change in forcing for the period 1870–2300, and an “A2 scenario” case in which both the amount of CO₂ in the atmosphere and the impact of that radiative forcing on the climate system are calculated based on the IPCC SRES (Nakicenovic and Swart 2000) A2 emission scenario (Houghton et al. 2001). Because the model has weaker climate sensitivity (Houghton et al. 2001), we choose A2, an aggressive emission scenario, in order to obtain a stronger climate change signal in the twenty-first century.

In the control case, climate drift for the period 1900–2300 is a -0.62-K ($\sim -0.15\text{ K century}^{-1}$) change in mean surface temperature (Table 1), a 3.8 ppmv increase in atmospheric CO₂ concentration, and an in-

TABLE 1. Changes in global- and annual-mean model results in coming centuries for the A2 scenario (e.g., decade of 1991–2000 minus 1891–1900 refers to the twentieth-century climate change). Percentage changes are computed relative to the decade of 1891–1900. All variables except CO₂ have been corrected for the drift in the control. For the TOA flux, changes are relative to the nineteenth century (e.g., decade of 2191–2200 minus 1891–1900 refers to the twenty-second-century climate change).

Period	Surface temperature (K)	Precipitation (%)	Water vapor (kg m ⁻²) (%)	Sea ice extent (%)	Sea ice volume (%)	CO ₂ (ppmv)	TOA flux (W m ⁻²)
Twentieth century	0.80	1.6	1.12 (5.3)	-7.4	-28.6	77	0.46
Twenty-first century	2.70	4.1	4.03 (19.0)	-25.1	-50.6	344	1.39
Twenty-second century	3.18	4.8	4.85 (22.8)	-42.6	-27.1	621	1.40
Twenty-third century	1.15	1.9	1.86 (4.1)	-15.0	-14.1	99	0.82
Total change	7.83	12.4	11.86 (52.2)	-90.1	-120.4	1141	0.82

crease of 8 gigatons of carbon (Gt C) in soil carbon. The drifts in sea ice area and volume for this 400-yr period are +15.3% and +40%, respectively. Relative to the size of the perturbation in our experiments, the drift in global mean temperature over 400 yr is small, yet sea ice is sensitive to this drift. In contrast, the carbon cycle model drift is over two orders of magnitude smaller than carbon cycle changes predicted in the A2 simulation.

In the A2 case, CO₂ emissions (Fig. 1) are specified at historical levels for the period 1870–2000 (see dataset

online at <http://cdiac.esd.ornl.gov/ndps/ndp030.html>) and at SRES A2 levels for the period 2000–2100 (Houghton et al. 2001). For the period 2100–2300, emissions follow a logistic function for the burning of the remaining fossil fuel resources (assuming 5270 Gt C in 1750; Caldeira and Wickett 2003; Metz et al. 2001). Non-CO₂ greenhouse gas concentrations are specified at historical levels for 1870–2000 and SRES A2 levels for 2000–2100 (Houghton et al. 2001) and are fixed at 2100 levels thereafter. Land-use emissions are taken from Houghton (2003) for the historical period and from the SRES A2 scenario for the period 2000–2100 and set to zero thereafter. There is no change in aerosol forcing. In this scenario, total emissions reach 30.8 Gt C yr⁻¹ around the year 2120 from present-day values of 8 Gt C yr⁻¹. The cumulative emission for the entire period 1870–2300 is 5404 Gt C. Total emissions in the twentieth, twenty-first, twenty-second, and twenty-third centuries are 385, 1791, 2558, and 644 Gt C, respectively; the rate of emissions peak in the twenty-second century for this scenario and the emission rates decline sharply in the twenty-third century.

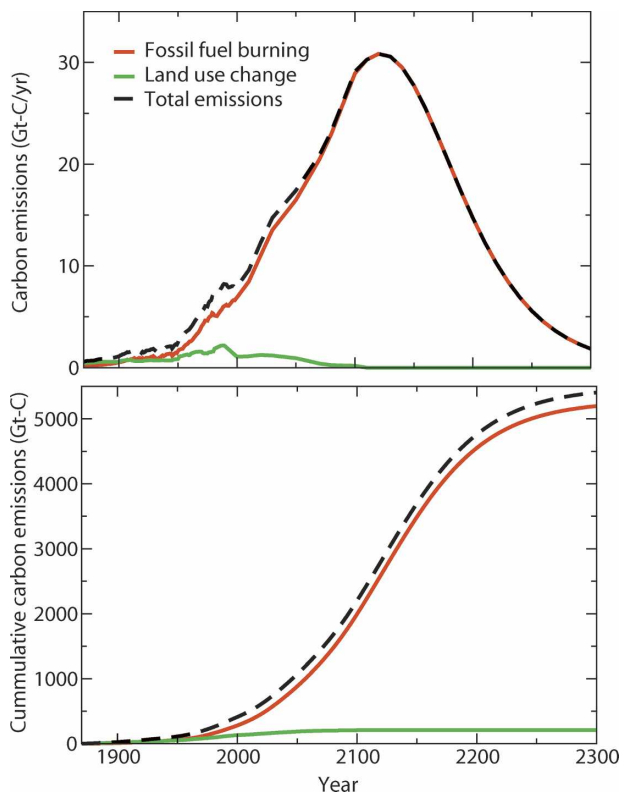


FIG. 1. Rate of (top) fossil fuel, land-use change, and total emissions and (bottom) cumulative emissions used in our simulations. Total emission rates reach peak values around the year 2120.

4. Results

a. Global climate change

The evolution of nondrift-corrected global and annual means of surface temperature and atmospheric CO₂ concentration is shown in Fig. 2. The modeled CO₂ concentration increases from the preindustrial value of 289 to 366 ppmv in the year 2000, suggesting that the modeled CO₂ is in good agreement with observations (Houghton et al. 2001). The surface temperature increases from 1870 to 2000 by about 0.8 K, which is also close to observations (Houghton et al. 2001). The fact that there is no change in aerosol forcing (i.e., absence of anthropogenic cooling from aerosols) in our experiments suggests that the model may be underestimating the warming. The global and annual mean transient

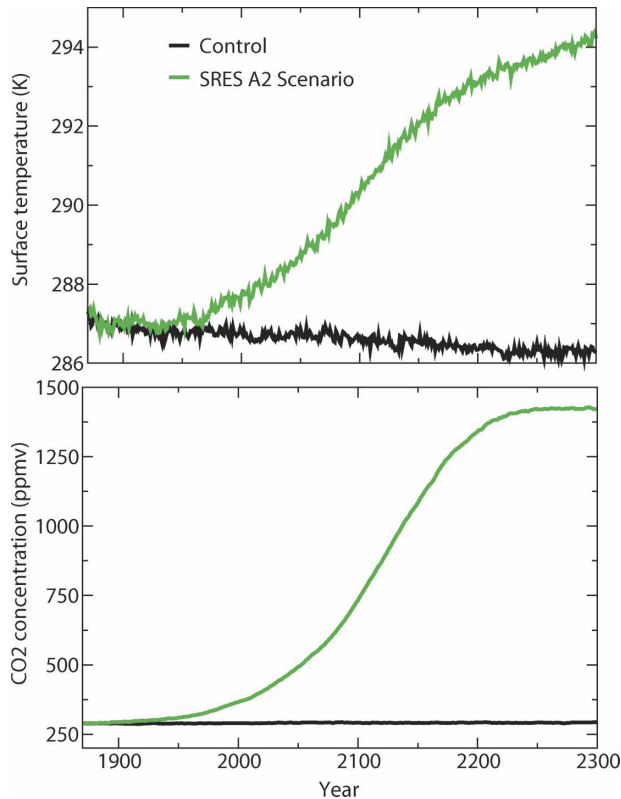


FIG. 2. Evolution of (top) global- and annual-mean surface temperature and (bottom) atmospheric CO_2 concentration. Surface temperature warming is about 8 K and atmospheric CO_2 concentration is 1423 ppmv at the year 2300.

climate responses are listed in Table 1. The climate drift from the control run is subtracted from our coupled run (Table 1). However, since the drift of the carbon cycle is negligible, we do not perform the subtraction for the carbon cycle variables. The global mean climate warms by 0.80, 2.7, 3.18, and 1.15 K in the twentieth, twenty-first, twenty-second, and twenty-third centuries, respectively (e.g., twentieth-century climate change refers to decade of 1991–2000 minus 1891–1900). The total warming from 1870 to 2300 is about 8 K. The warming is largest in the twenty-second century. Other responses like precipitation change, increase in atmospheric precipitable water, and decrease in sea ice extent are also largest in the twenty-second century when the emissions rates are the highest (Fig. 1).

The predicted atmospheric CO_2 concentration also shows the biggest increase in the twenty-second century (Table 1). However, the sea ice volume shows the fastest decline in the twenty-first century. Because of the large drift in sea ice (40% in 400 yr) the drift-corrected total change (Table 1) appears more than 100%, though the actual reduction was about 90%. We find that the sea ice cover disappears almost completely in

the Southern Hemisphere by the year 2150 during the Southern Hemisphere summers. An investigation into the causes of the climate drift in the climate model is beyond the scope of this paper.

The net radiative flux at the top of the atmosphere (TOA) increases to 1.39 W m^{-2} in the twenty-first century due to an increase in the heat content of the system. It is computed as the difference between net shortwave (absorption gain) and longwave (emission loss) fluxes at TOA. A positive (negative) net flux implies net gain (loss) of energy by the climate system. The equilibrium of the system is characterized by zero TOA net flux. The TOA net flux changes only by a little in the twenty-second century, to 1.40 W m^{-2} , suggesting very little additional gain of energy in the system in this century. In the twenty-third century, fossil fuel emission rates are declining and the climate system is gaining less energy than it gained before, as it moves toward equilibrium. The net energy gain from 1900 to 2300 is 0.82 W m^{-2} , suggesting that the system has not yet reached equilibrium in the year 2300 and will continue to warm.

We find that the depth of meridional overturning circulation (MOC) in the Atlantic becomes weak and shallow with climate change in this model, with much of the deep North Atlantic filling up with water from the Southern Ocean. For the preindustrial period and present day, the circulation at 24°N fills the whole depth, 5.5 km, of the North Atlantic Ocean. The depth of MOC is defined as the distance from the surface to where the water transport becomes zero. By the year 2100, the depth of MOC is reduced to 3 km. It is reduced further to 2 km by the year 2300. We also find that the amplitude of the Atlantic MOC shows nearly 45% weakening [32 to 18 Sv ($1 \text{ Sv} \equiv 10^6 \text{ m}^3 \text{ s}^{-1}$)] by the year 2100 and it does not show a significant decline afterward. Our model-simulated Atlantic MOC in the control climate has an amplitude that is larger than observations (19.3 Sv in Hall and Bryden 1982; Nof 2002). Our model is among the climate models that simulate stronger MOC (Houghton et al. 2001). However, the fractional decline in MOC in our model in response to warming by the year 2100 is comparable to other models.

Figure 3 shows the evolution of radiative forcing and the global- and annual-mean surface temperature change as a function of radiative forcing in our coupled A2 simulation. Radiative forcing is defined as the instantaneous change in net radiative flux at the tropopause, adjusted for stratospheric relaxation, due to some external forcing such as an increase in greenhouse gases. We used the formulas from Houghton et al. (1997) for the computation of radiative forcing of CO_2 and other non- CO_2 greenhouse gases, and adopted a

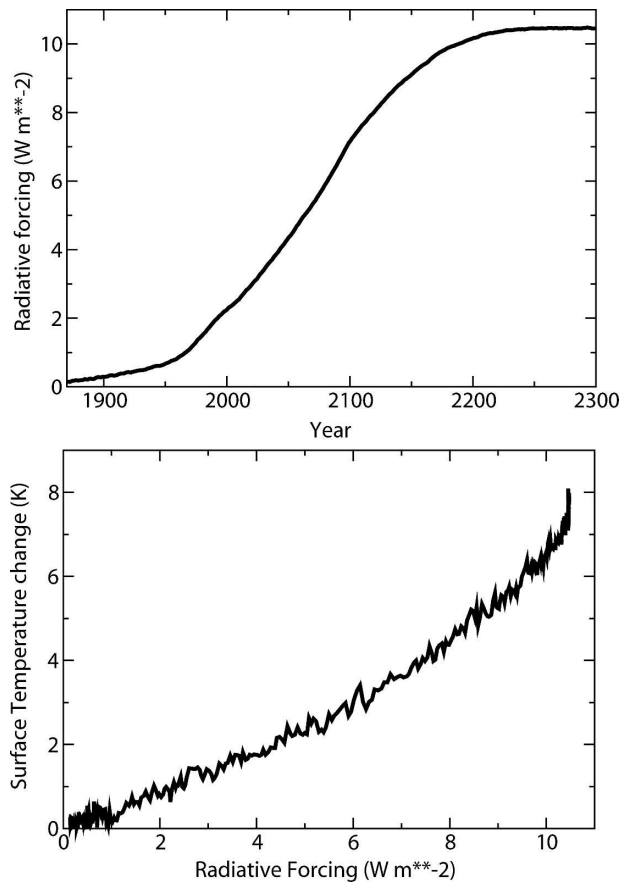


FIG. 3. Evolution of (top) radiative forcing and (bottom) the global- and annual-mean surface temperature change in the coupled A2 simulation as a function of radiative forcing. The amount of warming is much larger during the second half of the forcing than in the first half because of the thermal lag of the climate system and an increase in climate sensitivity with time (or warming).

value of 3.45 W m^{-2} for the radiative forcing due to a doubling of CO_2 in this model. The “equilibrium climate sensitivity” of the model is known to be 2.1 K per doubling of CO_2 using a slab ocean model (Houghton et al. 2001). The equilibrium climate sensitivity is defined as the warming obtained due to a doubling of CO_2 when the climate system comes to complete equilibrium. Since a full ocean model takes multiple centuries to reach equilibrium, the equilibrium climate sensitivity value is usually obtained from performing slab ocean experiments for a few decades.

Because of the thermal inertia of the oceans, the surface temperature has warmed only 2.25 K when the radiative forcing is 5 W m^{-2} (Fig. 3b). However, the warming becomes 8 K when the radiative forcing reaches about 10.5 W m^{-2} . The larger warming in the latter half of the radiative forcing can be partly explained by the thermal lag of the climate system. It is

also due partly to the increase of “effective climate sensitivity” as the simulation progresses (Fig. 4; Senior and Mitchell 2000; Gregory et al. 2004); a radiative forcing of about 10.5 W m^{-2} would suggest an equilibrium warming of 6.3 K for this model, assuming an equilibrium climate sensitivity of 2.1 K. However, the warming is 8 K and the climate system has not reached equilibrium yet. It is likely there will be further warming with no further increase in forcing (Fig. 3b) because of the thermal lag of the coupled climate system. Therefore, the warming is larger than expected from the results of single-century simulations or equilibrium simulations using a slab ocean version of the model.

The climate sensitivity plotted in Fig. 4 is the effective climate sensitivity as defined in Murphy (1995) and Senior and Mitchell (2000). The effective climate sensitivity at any time can be thought of as “the climate sensitivity per doubling of CO_2 that would occur if

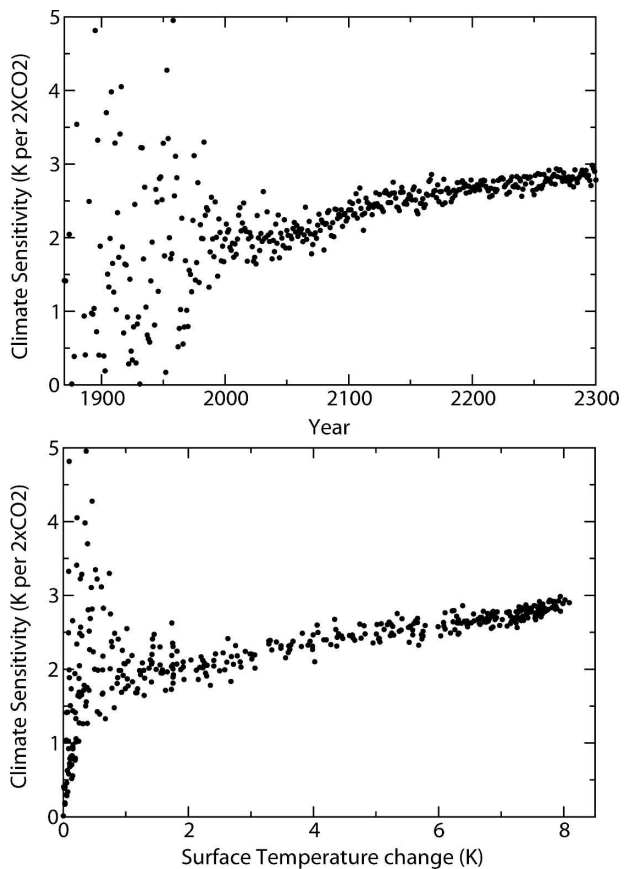


FIG. 4. “Effective” climate sensitivity as a function of (top) time and (bottom) surface temperature change. Here, climate sensitivity is defined as the amount of warming per doubling of CO_2 . The signal-to-noise ratio is much improved after the year 2050 (or after a warming of 2 K). Climate sensitivity is seen to increase from about 2 to 3 K as the simulation progresses, an increase of about 50%.

the climate model ran to equilibrium with feedback strengths held fixed at the values diagnosed at that time during the run.” The signal-to-noise ratio is much improved (Fig. 4) after the year 2050 (or after a warming of 2 K). The effective climate sensitivity is seen to increase from the model’s previously known equilibrium value of about 2–3 K, an increase of about 50%. Senior and Mitchell (2000) found that the effective climate sensitivity of their coupled system increased by 40% in an 800-yr integration, and the time dependence was associated with differences in cloud feedback arising from interhemispheric temperature differences due to the slower warming rate of the Southern Ocean.

The coupled system’s effective climate sensitivity is close to the equilibrium climate sensitivity (2.1 K) as estimated using a slab ocean model up to the year 2100. Therefore, the use of equilibrium climate sensitivity from a slab ocean experiment may be a good approximation to the coupled system’s sensitivity in many recent coupled climate-modeling studies that have focused on climate change over the twenty-first century. However, it may underestimate the long-term (multi-century) climate change due to greenhouse gas emissions. The likely causes for the increase in climate sensitivity in our model are changes in cloud feedback, radiative forcing, ocean heat transport, and vegetation distribution. While the effective climate sensitivity in Senior and Mitchell (2000) increases toward the equilibrium climate sensitivity value as the warming progresses, in our study it starts out at the equilibrium value and increases by 50% above that value. An investigation into the increase of effective climate sensitivity with time (or warming) in our model will be the subject of a future paper.

b. Land and ocean carbon fluxes

The 5-yr running mean of global and annual mean net land and ocean uptakes are shown in Fig. 5. For the 30 yr centered on 1985, the mean land and ocean uptake of carbon are 3.0 and 1.3 Gt C yr⁻¹, respectively. Compared to the observational estimates of land and ocean fluxes for the 1980s of 0.2 ± 0.7 and 1.9 ± 0.6 Gt C yr⁻¹ and for the 1990s of 1.4 ± 0.7 and 1.7 ± 0.5 Gt C yr⁻¹ (Prentice et al. 2000, 2001), the model tends to overestimate historical terrestrial carbon uptake and underestimate oceanic uptake. The land uptake increases monotonically with time until year 2120 when the uptake is about 45% of the total emissions. The effect of CO₂ fertilization is probably exaggerated in our simulation because we do not consider factors other than limitation by sunlight, water, and carbon dioxide. Compared to similar models, IBIS2 tends to simulate a higher fertilization effect (Mc Guire et al. 2001). Land

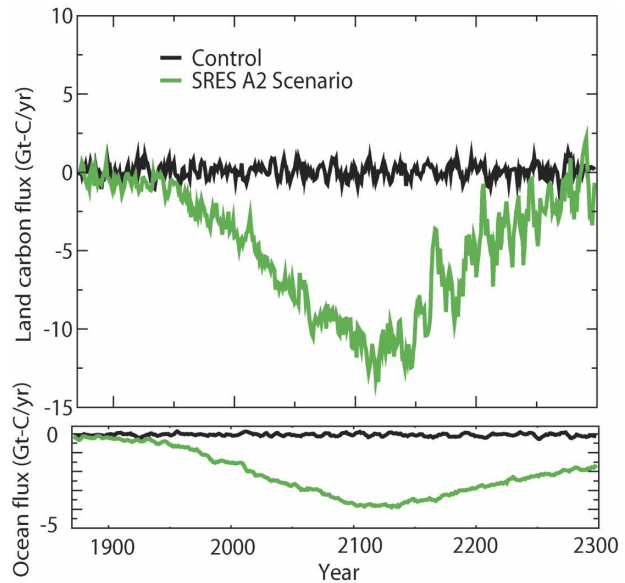


FIG. 5. Evolution of the 5-yr running mean of global, annual flux of carbon from (top) land to atmosphere and (bottom) ocean to atmosphere. Negative values represent fluxes into land and ocean. Land fluxes show a dramatic reversal after the year 2100 and ocean fluxes also decrease slightly after the year 2100.

uptake of carbon starts to decline in the twenty-second century when the emissions rates also begin to decrease. By the year 2300, it reaches levels close to zero because increased heterotrophic respiration (Fig. 6) offsets NPP.

Net land uptake is mainly NPP minus heterotrophic respiration (RH). The ecosystem disturbances such as fire are parameterized as CO₂ sources to the atmosphere and their magnitude is only about 10% of NPP or RH. NPP and RH show sharp increases during 2000–2150 and remain steady thereafter (Fig. 6, top panel). The land uptake is mostly stored in biomass (Fig. 6, middle panel). The increase in the amount of biomass carbon from its preindustrial value of about 700 Gt C is about 1300 Gt C by the year 2300. However, soil carbon shows only a modest increase of about 500 Gt C because of a sharp fall in its turnover time (Fig. 6, bottom panel). The turnover times of biomass and soil carbon are obtained by dividing their masses by NPP and RH, respectively. The newly produced carbon in the soil pool is labile, and hence the turnover time of soil carbon is sharply reduced by the year 2150 (Fig. 6, bottom panel). Neither soil carbon nor biomass shows any decline during the entire simulation (Fig. 6, middle panel), and the land remains a sink for carbon throughout our A2 simulation (Fig. 5). However, a higher climate sensitivity could result in significantly increased soil microbial respiration and a decline in soil carbon (Govin-

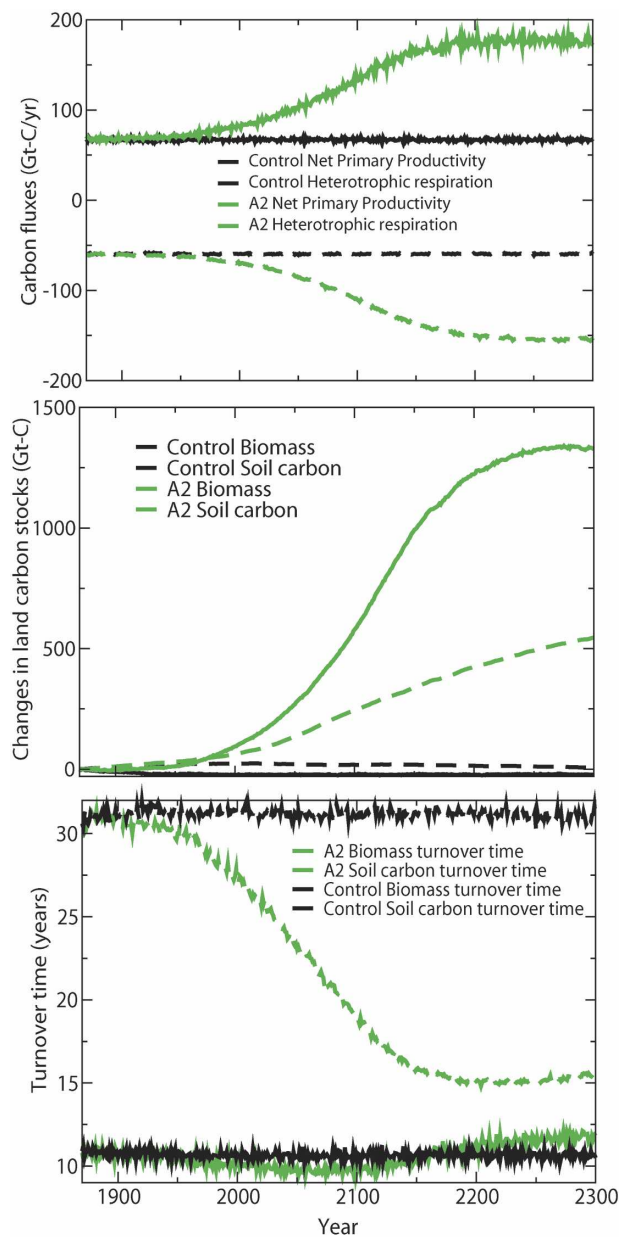


FIG. 6. Evolution of (top) NPP and heterotrophic (soil microbial) respiration, (middle) changes in vegetation biomass and soil carbon content, and (bottom) the turnover time of the biomass and soil carbon pools. Though the turnover time of soil carbon declines dramatically, it does not become smaller than the turnover time of biomass; hence, the land always remains a net sink.

dasamy et al. 2005). If there is no additional CO_2 fertilization after the year 2000 level, then the soil carbon content could be declining by the year 2100 (Thompson et al. 2004).

The ocean uptake increases to about 4 Gt C yr^{-1} , peaking after the year 2100, following the pattern of CO_2 emissions to the atmosphere (Fig. 5). The uptake

reaches only a third of the land uptake. This may be an underestimate, as the model tends to underestimate historical ocean carbon uptake estimates (Prentice et al. 2001; Sabine et al. 2004) and model results from OCMIP (Orr and Dutay 1999; Orr et al. 2001). Like the land uptake, the ocean uptake also declines in the twenty-second and twenty-third centuries when the emissions rates are decreasing. This decrease in uptake is due to the warming of the surface ocean that drives enhanced CO_2 fluxes out of the ocean (Sarmiento and Le Quere 1996; Sarmiento et al. 1998). Since the ocean time scales for reaching equilibrium are much higher than land time scales (Kheshgi 2004), the ocean uptake in the year 2300, unlike the land uptake, has not yet reached equilibrium though the emission rates are nearly zero in the year 2300. Therefore, the ocean continues to draw down CO_2 beyond the year 2300.

c. Carbon cycle feedback factor

The “carbon cycle feedback factor” is defined as the ratio of CO_2 change when climate is changing to the CO_2 change when the climate is constant (Friedlingstein et al. 2003). Here, it is the ratio between the CO_2 change in our A2 experiment and that in a zero climate sensitivity experiment. In the zero climate sensitivity experiment, the land and ocean carbon cycle models perceive the emissions and predicted atmospheric CO_2 content, but the climate system perceives the preindustrial values of CO_2 and other greenhouse gases. We extended the zero climate sensitivity experiment of Thompson et al. (2004) and Govindasamy et al. (2005) to the year 2300. The carbon cycle feedback factor may depend on the carbon cycle processes (Thompson et al. 2004) and climate sensitivity to greenhouse gases (Govindasamy et al. 2005).

The implied net carbon cycle feedback factor in our simulations is 1.09 between 1870 and 2000 (Table 2). It increases to 1.13 for the period between 1870 and 2100. The net carbon cycle feedback factors are 1.19, 1.675, 1.24, and 1.2 for the same period in Friedlingstein et al.

TABLE 2. Carbon cycle feedback factors for the periods from the years 2000, 2100, 2200, and 2300. Predicted CO_2 values are listed for the years 1870, 2000, 2100, 2200, and 2300.

Yr	CO_2 in uncoupled run (ppmv)	CO_2 in coupled A2 scenario (ppmv)	Carbon cycle feedback factor
1870	289	289	—
2000	360	366	1.09
2100	681	732	1.13
2200	1155	1341	1.22
2300	1166	1423	1.29

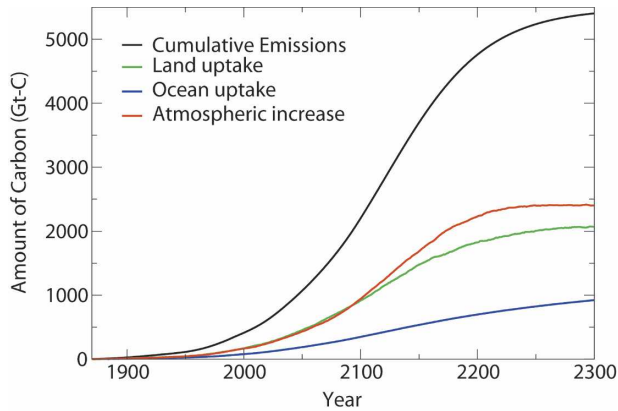


FIG. 7. Evolution of cumulative carbon emissions, uptakes by land and oceans, and the amount of carbon that stays in the atmosphere since the preindustrial period in the fully coupled experiment.

(2001), Cox et al. (2000), Zeng et al. (2004), and Mathews et al. (2005), respectively. Therefore, our model shows the weakest feedback between climate and carbon cycle among the existing coupled climate and carbon cycle models. The feedback factor increases to 1.29 for 1870–2300, the entire period of simulation. We believe that this increase is due to the reduction in the turnover time scale of the soil carbon pool with time (Fig. 6c), and because of an increase in climate sensitivity with time (see the discussion for Figs. 3 and 4). However, the increase in the feedback factor is small and it suggests near-linear behavior of the carbon cycle feedback factor over the 430-yr period.

d. Fate of anthropogenic emissions

Under the SRES A2 scenario, the total emission rate reaches $30.8 \text{ Gt C yr}^{-1}$ at the year 2120. The cumulative anthropogenic emission for the period 1870–2300 is 5404 Gt C. The amounts taken up by land and ocean are shown in Fig. 7. By 2300, the land biosphere takes up 2067 Gt C, nearly 38% of the emissions. During the same period, oceans take 921 Gt C or 17% of the emissions. The residual, 2416 Gt C (45%) stays in the atmosphere. The uptake fractions depend on the amount of global warming; land uptake decreases from 47% to

29% of the total emissions as the global temperature change increases from 0 to 8 K in our model (Govindasamy et al. 2005). It also depends on other assumptions; Thompson et al. (2004) demonstrated that terrestrial biosphere could become a source of carbon to the atmosphere by the year 2050 if nitrogen/nutrient limitations limit CO_2 fertilization levels to that of the year 2000.

The partitioning of the emissions between the reservoirs (land, ocean, and atmosphere) by century shows that the land and atmosphere take about 40% each of the emissions and the ocean takes up about 20% in the twentieth century (Table 3). The emissions and the uptakes by all reservoirs increase in the twenty-first century and reach peak values in the twenty-second century, and they then show sharp declines in the twenty-third century. Fractional terrestrial uptake declines in the twenty-second and twenty-third centuries presumably because of a warmer climate. Fractional oceanic uptake becomes smallest in the twenty-second century when the emissions rates are the highest, even though the absolute amount of uptake is the largest for oceans. The slower response due to long ocean time scales is responsible for this behavior. Fractional atmospheric uptake reaches its peak value of 50% in the same period. It decreases to 27% in the twenty-third century. Fractional oceanic uptake increases to 35% in the twenty-third century, suggesting the role of the oceans in the eventual uptake of anthropogenic emissions.

e. Changes in vegetation distribution

Dominant vegetation distributions from our simulations for the periods 1971–2000, 2071–2100, 2171–2200, and 2271–2300, designated as twentieth-, twenty-first-, twenty-second-, and twenty-third-century vegetation distribution, respectively, are shown in Fig. 8. Maps of vegetation distributions are compared using kappa statistics (Monsrud 1990). The kappa value equals 1 with perfect agreement, and it is close to 0 when the agreement is approximately the same as would be expected by chance. Foley et al. (1996) obtain a kappa value of 0.47 (fair agreement; Landis and Koch 1977) for a comparison of IBIS2-simulated vegetation and observations

TABLE 3. Total emissions (Gt C) and its partitioning between various reservoirs for each century. Numbers in brackets represent the percent of the partitioning.

Reservoir	Twentieth century	Twenty-first century	Twenty-second century	Twenty-third century	Total since 1870
Emissions	385.1	1790.6	2557.6	644.7	5404
Land	160.7 (41.7)	746.8 (41.7)	906.4 (35.4)	243.9 (37.8)	2067 (38.3)
Ocean	71.7 (18.6)	269.2 (15.0)	350.0 (13.7)	224.4 (34.8)	921 (17.0)
Atmosphere	153.0 (39.7)	777.2 (43.3)	1289.0 (50.9)	174.0 (27.4)	2416 (44.7)

Dominant Vegetation Types

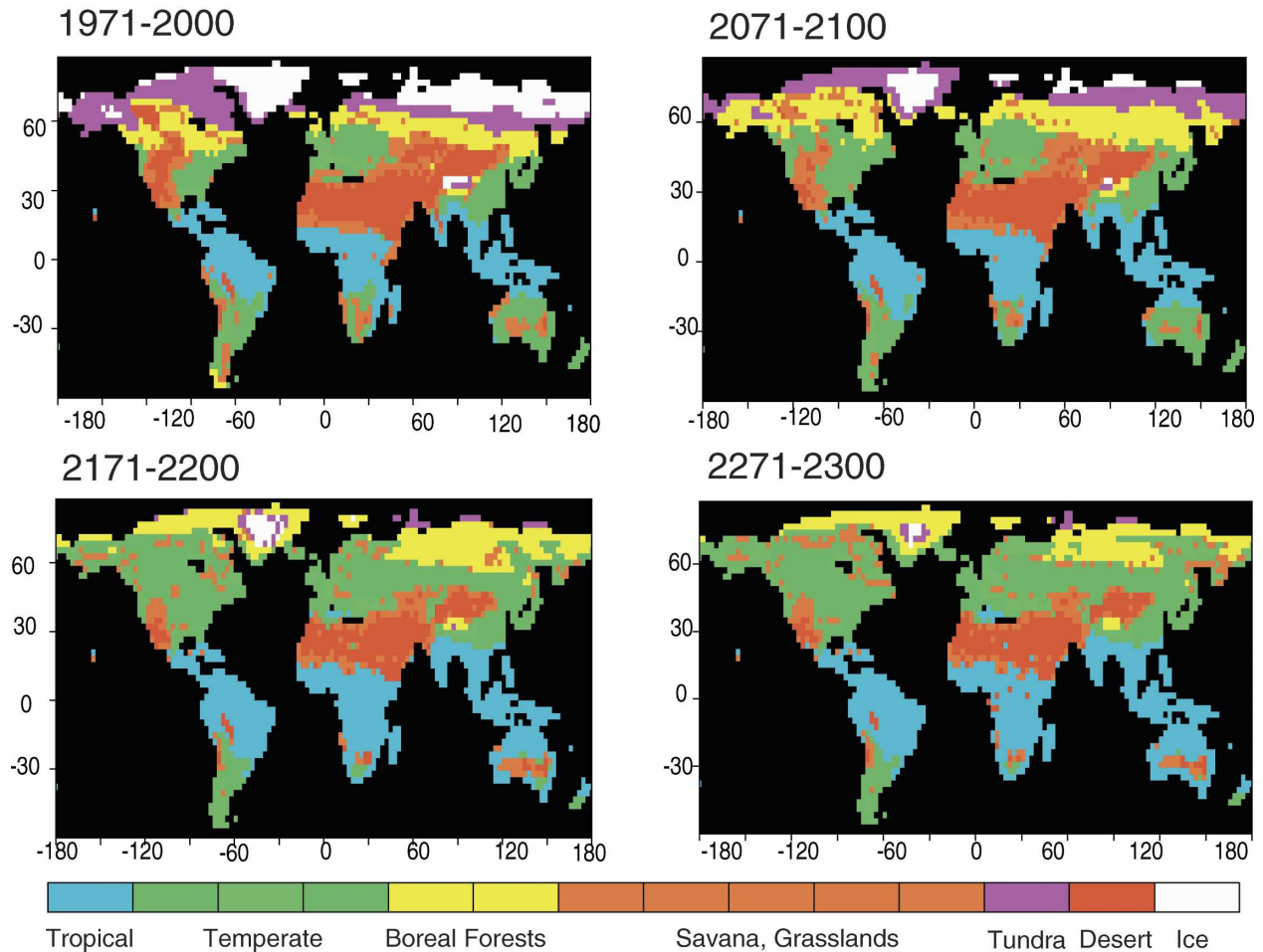


FIG. 8. Vegetation distributions in our simulations. Antarctica is not shown. The area covered by tropical and temperate forests increases dramatically when global warming increases by the year 2300. There is also a migration of tropical, temperate, and boreal forests poleward with warming, leading to significant declines in area occupied by tundra and polar deserts (land ice).

(Foley et al. 1996). A kappa value of 0.41 (fair) is obtained when we compare our model-simulated preindustrial vegetation with potential natural vegetation. Potential natural vegetation represents the vegetation that would exist in a location in the absence of human intervention and is derived from a study by Ramanakutty and Foley (1999). The INCCA model simulates too much forest cover in South America, Africa, and Australia, at the expense of grassland, shrubland, and savannas. The northern tree line and the northern vegetation limit (tundra/land ice) are also simulated too far south in Asia due to a cold bias in the region.

Global comparisons of simulated twentieth-century vegetation distributions with distributions of twenty-first, twenty-second, and twenty-third centuries give kappa values of 0.61 (good agreement), 0.40 (fair), and 0.32 (poor), respectively. In terms of the area occupied

by different vegetation types, tropical and temperate forests expand significantly with global warming (Fig. 8; Table 4). The area covered by those forests increases from about 45% in the twentieth century to nearly 65% of the land area in the twenty-third century. In general there is an expansion of tropical forest poleward, a migration and expansion of temperate forest poleward, and a migration of boreal forest poleward, leading to significant declines in the area occupied by tundra and polar deserts (land ice). By the year 2300, most of North America and to a lesser extent Eurasia are covered by temperate forest while boreal forest is limited to northern Siberia and Greenland. The timing of the forest expansion in Greenland might not be realistic because IBIS2 does not include a proper ice sheet model and the vegetation dynamics module does not take into account soil formation processes. However,

TABLE 4. Fraction of land area occupied by vegetation types at the end of centuries (e.g., twentieth-century vegetation refers to the dominant vegetation during 1971–2000).

Vegetation type	Twentieth century	Twenty-first century	Twenty-second century	Twenty-third century
Tropical forests	22.9	24.6	32.8	34.1
Temperate forests	21.1	24.3	29.7	30.5
Boreal forests	7.9	10.6	7.4	7.0
Savanna, grassland, and shrubland	11.8	11.8	10.1	10.2
Tundra	7.7	6.5	2.7	1.8
Desert	15.3	12.3	11.3	11.6
Polar desert	13.3	7.9	6.0	4.8

there is evidence of a partly forested Greenland during the Holocene and mostly the Eemian (Bennike and Bocher 1994, 1990).

Interestingly, the fraction of deserts shows a decline of about 4% by the year 2300. The comparison with the zero climate sensitivity experiment shows that the reduction of the desert is due in part to higher water-use efficiency under higher atmospheric CO₂ concentration but also to increased precipitation in the border regions. Tropical forest expansion is also partly due to the CO₂ fertilization effect but mostly to increased precipitation in the Tropics. The expansion of temperate forest over all of North America and most of Eurasia is favored by higher CO₂ but is mainly due to the warming of the midlatitudes. The reduction in the area covered by land ice and tundra on the other hand is mostly due to warming. The large increase in biomass (Fig. 6, middle panel) and hence the land carbon uptake (Table 3; Figs. 5 and 7) is due to the direct fertilization effect of CO₂, with ecosystems accumulating more biomass, but also to vegetation dynamics, with forested ecosystems with higher biomass replacing grasslands, shrubland, and tundra. These results do not take into account the constraint land use puts on the development of natural ecosystems. In our simulations, we only account for the global carbon emissions due to land use by using Houghton's (2003) estimate for the historical period, the SRES A2 scenario for the period 2000–2100 and zero thereafter. We do not actually simulate crops with IBIS2 and the model setup allows natural vegetation to grow everywhere. However, forests will not be able to grow as simulated here because a large part of the land surface will be under some form of cultivation (Ramanakutty et al. 2002). This would limit carbon uptake by the land biosphere because most cultivated ecosystems do not accumulate biomass, and under current management practices, very little litter enters the soil. In summary, Fig. 8 shows only the potential vegetation distributions at the end of each century; it does not include the human-induced land-use changes. We also caution that climate change and CO₂ fertilization could also

impact ecosystem goods and services not represented by our terrestrial ecosystem model, such as species abundance and competition, seed dispersal, habitat loss, biodiversity, and other disturbances (Root and Schneider 1993).

5. Discussion

In this paper, we have investigated global climate change and the carbon budget out to the year 2300 that would occur if CO₂ emissions from all the currently estimated fossil fuel resources were released to the atmosphere. Emissions from the SRES A2 scenario are used to the year 2100. For the period 2100–2300, emissions follow a logistic function for the burning of the remaining fossil fuel resources. In our emission scenario, it is assumed that about 5000 Gt C is available as fossil fuel in the year 2000 (with about 270 Gt C emitted before then). In our model, the climate warms by 8 K by the year 2300. This warming is higher than anticipated because of an increase in climate sensitivity as the simulation progresses. Of the total fossil fuel and land-use change emissions of 5400 Gt C for the period 1870–2300, about 38% and 17% are taken up by land and oceans, respectively, and the remaining 45% stays in the atmosphere. Atmospheric CO₂ concentrations are 257 ppmv higher in the fully coupled simulation than in the no-climate change run. The carbon cycle feedback factor shows an increase from 1.09 to 1.29 when global warming increases from 0.8 in the year 2000 to 8 K in the year 2300. Even though our model has relatively lower climate sensitivity among the climate models (Houghton et al. 2001) and weak carbon cycle feedback, our results suggest severe long-term consequences for global climate if CO₂ emissions from all the currently estimated fossil fuel resources were released to the atmosphere.

The land model IBIS2 has a vigorous CO₂ fertilization effect and hence the terrestrial uptake is overestimated for the historical period, and possibly for the future as well. Our model has weak climate–carbon

cycle feedback and the predicted atmospheric CO₂ is relatively lower in comparison to other coupled climate–carbon cycle models for the twenty-first century (Friedlingstein et al. 2001; Cox et al. 2000; Zeng et al. 2004; Mathews et al. 2005). Our physical climate model has relatively lower climate sensitivity among the climate models (Houghton et al. 2001). Given these facts, our model simulation represents a conservative estimate of how the specified emissions could affect climate in the future.

Our land carbon cycle model remains a net sink for carbon in the atmosphere even when the warming is as high as 8 K at the year 2300. In the third Hadley Centre Coupled Ocean–Atmosphere General Circulation Model (HadCM3; Cox et al. 2000; 2004; Betts et al. 2004), carbon in Amazonian vegetation begins to decline by the year 2050, as a drying and warming of Amazonia initiates forest loss. Such a loss of vegetation biomass does not occur in our simulations. In our simulation, soil carbon increases throughout the simulation. However, either less CO₂ fertilization or higher climate sensitivity could result in increased soil microbial respiration and a decreased soil carbon reservoir in this model (Govindasamy et al. 2005; Thompson et al. 2004). The dieback of the Amazon in Cox et al. (2000, 2004) is a distinctive feature of the pattern of climate change simulated by HadCM3; Cramer et al. (2004) showed that this vegetation change does not occur when the land model [Top-down Representation of Interactive Foliage and Flora Including Dynamics (TRIFID)] in HadCM3 is forced by the output from other climate models.

In the real world, as opposed to our model, CO₂-fertilized ecosystems may run into nutrient limitations. The high sensitivity of our terrestrial biosphere model to added CO₂ might be associated with the lack of nutrient cycles (e.g., nitrogen, phosphorous, etc.). Changes in nitrogen availability are important to the carbon cycle through changes in plant nutrient availability (Field et al. 1995; Schimel 1998; Nadelhoffer et al. 1999; Shaw et al. 2002; Hungate et al. 2003). Models that include nitrogen limitation show less sensitivity of CO₂ fluxes for changes in atmospheric CO₂ (Cramer et al. 2001). Oren et al. (2001) and Nowak et al. (2004) found that nutrient limitations could slow NPP response to rising CO₂ but not stop it. Even without nutrient limitations, the enhanced physiological effects of CO₂ on productivity and water-use efficiency asymptote at high CO₂ concentrations (Farquhar et al. 1980; King et al. 1997; Cao and Woodward 1998). Our terrestrial biosphere model also lacks acclimation of soil microbiology to higher temperatures (Kirschbaum 2000; Tjoelker et al. 2001). We have not simulated re-

alistic land use in order to correctly account for the differences between crops and natural ecosystems.

As in most carbon cycle–climate studies, we assumed constant aerosol forcing in our simulations. If all fossil fuel reserves are to be used by the year 2300, it is likely that oil and gas burning will be replaced by coal burning, with coal reserves being much larger than oil and natural gas (International Energy Outlook 2004). In addition, the switch from oil and gas burning to coal burning is likely to be associated with changes in aerosol emissions, as well as methane and black carbon emissions. The net effect of these changes is hard to estimate as they depend on the type of coal and on the development and availability of clean technology. It is likely however that the overall effect will accelerate warming. In a reverse study, Hayhoe et al. (2002) showed that a switch from coal to natural gas in the utility sector could result in an initial warming phase followed by a cooling trend. The initial warming is due to the decrease of SO₂ emissions and the following decrease to the lower emissions of CO₂ and black carbon.

Our coupled climate–carbon-modeling study indicates that the carbon cycle feedback factor and the fraction of anthropogenic CO₂ that stays in the atmosphere will slightly increase as the planet warms. Our previous studies (Thompson et al. 2004; Govindasamy et al. 2005) using this model have shown that the future accumulation of atmospheric CO₂ is sensitive to terrestrial carbon cycle processes (e.g., CO₂ fertilization and respiration) and climate sensitivity to CO₂, about which we are uncertain at present. These uncertainties could perhaps be narrowed with investigation of carbon dynamics across a broad range of ecosystems and climate regimes, often including manipulation experiments, and redoubled efforts to represent those dynamics in climate models.

Because of the limitations of the model and the unknowns linked to technological advances, the future of land use, and demography in the next 200 yr, our study is mostly a sensitivity study. However, it shows that both climate sensitivity to radiative forcing and carbon cycle feedback with climate increase with time. As our model tends to have low climate sensitivity to radiative forcing and a small feedback between the carbon cycle and the climate, our model projections indicate the potential for severe long-term consequences for global climate if all the fossil fuel carbon is ultimately released to the atmosphere.

Acknowledgments. This work was performed under the auspices of the U.S. Department of Energy by the University of California Lawrence Livermore National Laboratory under Contract W-7405-Eng-48. We thank

Drs. Michael Notaro and Dammon Matthews for helpful comments on an earlier version of the manuscript.

REFERENCES

- Amthor, J. S., 1984: The role of maintenance respiration in plant growth. *Plant Cell Environ.*, **7**, 561–569.
- Bennike, O., and J. Bocher, 1990: Forest–tundra neighbouring the North Pole: Plant and insect remains from the Pliocene–Pleistocene Kap Kobenhavn formation, north Greenland. *Arctic*, **43**, 331–338.
- , and —, 1994: Land biotas of the last interglacial/glacial cycle on Jameson Land, East Greenland. *Boreas*, **23**, 479–487.
- Betts, R. A., P. M. Cox, M. Collins, P. Harris, C. Huntingford, and C. D. Jones, 2004: The role of ecosystem–atmosphere interactions in simulated Amazonian precipitation decrease and forest dieback under global warming. *Theor. Appl. Climatol.*, **78**, 157–175.
- Caldeira, K., and M. Wickett, 2003: Oceanography: Anthropogenic carbon and ocean pH. *Nature*, **425**, 365.
- Cao, M., and F. I. Woodward, 1998: Dynamic responses of terrestrial ecosystem carbon cycling to global climate change. *Nature*, **393**, 249–252.
- Cramer, W., and Coauthors, 2001: Global response of terrestrial ecosystem and function to CO₂ and climate change: Results from six dynamic global vegetation models. *Global Change Biol.*, **7**, 357–373.
- , A. Bondeau, S. Schaphoff, W. Lucht, B. Smith, and S. Sitch, 2004: Tropical forests and the global carbon cycle: Impacts of atmospheric carbon dioxide, climate change and rate of deforestation. *Philos. Trans. Roy. Soc. London*, **359**, 311–343.
- Collatz, G. J., J. T. Ball, C. Grivet, and J. A. Berry, 1991: Physiological and environmental regulation of stomatal conductance, photosynthesis and transpiration: A model that includes a laminar boundary layer. *Agric. For. Meteorol.*, **53**, 107–136.
- , M. Ribas-Carbo, and J. A. Berry, 1992: Coupled photosynthesis–stomatal conductance model for leaves of C₄ plants. *Aust. J. Plant Physiol.*, **19**, 519–538.
- Cox, P. M., R. A. Betts, C. D. Jones, S. A. Spall, and I. J. Totterdell, 2000: Acceleration of global warming due to carbon-cycle feedbacks in a coupled model. *Nature*, **408**, 184–187.
- , —, M. Collins, P. P. Harris, C. Huntingford, and C. D. Jones, 2004: Amazonian forest dieback under climate–carbon cycle projections for the 21st century. *Theor. Appl. Climatol.*, **78**, 137–156.
- Curtis, P. S., 1996: A meta-analysis of leaf gas exchange and nitrogen in trees grown under elevated carbon dioxide. *Plant Cell Environ.*, **19**, 127–137.
- Dukowicz, J. K., and R. D. Smith, 1994: Implicit free-surface method for the Bryan–Cox–Semtner ocean model. *J. Geophys. Res.*, **99**, 7991–8014.
- Farquhar, G. D., S. V. Caemmerer, and J. A. Berry, 1980: A biochemical-model of photosynthetic CO₂ assimilation in leaves of C-3 species. *Planta*, **149**, 78–90.
- Field, C., R. Jackson, and H. Mooney, 1995: Stomatal responses to increased CO₂: Implications from the plant to the global scale. *Plant Cell Environ.*, **18**, 1214–1225.
- Foley, J. A., I. C. Prentice, N. Ramankutty, S. Levis, D. Pollard, S. Sitch, and A. Haxeltine, 1996: An integrated biosphere model of land surface processes, terrestrial carbon balance and vegetation dynamics. *Global Biogeochem. Cycles*, **10**, 603–628.
- Friedlingstein, P., L. Bopp, P. Ciais, J. L. Dufresne, L. Fairhead, H. LeTruet, P. Monfray, and J. Orr, 2001: Positive feedback between future climate change and the carbon cycle. *Geophys. Res. Lett.*, **28**, 1543–1546.
- , J.-L. Dufresne, P. M. Cox, and P. Rayner, 2003: How positive is the feedback between climate change and the carbon cycle? *Tellus*, **55B**, 692–700.
- Govindasamy, B., S. Thompson, A. Mirin, M. Wickett, K. Caldeira, and C. Delire, 2005: Increase of carbon cycle feedback with climate sensitivity: Results from a coupled climate and carbon cycle model. *Tellus*, **57B**, 153–163.
- Gregory, J. M., and Coauthors, 2004: A new method for diagnosing radiative forcing and climate sensitivity. *Geophys. Res. Lett.*, **31**, L03205, doi:10.1029/2003GL018747.
- Hall, M. M., and H. L. Bryden, 1982: Direct estimates of ocean heat transport. *Deep-Sea Res.*, **29**, 339–359.
- Hayhoe, K., H. S. Khesghi, A. K. Jain, and D. J. Wuebbles, 2002: Substitution of natural gas for coal: Climatic effects of utility sector emissions. *Climate Change*, **54**, 107–139.
- Houghton, J. T., L. G. Meira Filho, D. J. Griggs, and K. Maskell, Eds., 1997: An introduction to simple climate models used in the IPCC second assessment report. IPCC Tech. Paper II, IPCC, Geneva, Switzerland, 54 pp. [Available online at <http://www.undp.org/cc/pdf/Help%20Desk/IPCCtechpap2.pdf>.]
- , Y. Ding, D. J. Griggs, M. Noguer, P. J. van der Linden, X. Dai, K. Maskell, and C. A. Johnson, Eds., 2001: *Climate Change 2001: The Scientific Basis*. Cambridge University Press, 881 pp.
- Houghton, R., 2003: Revised estimates of the annual net flux of carbon to the atmosphere from changes in land use and land management 1850–2000. *Tellus*, **55B**, 378–390.
- Hungate, B. A., J. S. Dukes, M. R. Shaw, Y. Luo, and C. B. Field, 2003: Nitrogen and climate change. *Science*, **302**, 1512–1513.
- Energy Information Administration, 2004: International energy outlook 2004. Office of Integrated Analysis and Forecasting, U.S. Department of Energy Rep. DOE/EIA-0484, Washington, DC, 244 pp.
- Joos, F., I. C. Prentice, S. Sitch, R. Meyer, G. Hooss, G.-K. Plattner, S. Gerber, and K. Hasselmann, 2001: Global warming feedbacks on terrestrial carbon uptake under the Intergovernmental Panel on Climate Change (IPCC) emission scenarios. *Global Biogeochem. Cycles*, **15**, 891–907.
- Khesghi, H. S., 2004: Ocean carbon sink duration under stabilization of atmospheric CO₂—A 1000-year time scale. *Geophys. Res. Lett.*, **31**, L20204, doi:10.1029/2004GL020612.
- Kiehl, J. T., J. J. Hack, G. B. Bonan, B. Y. Boville, B. P. Briegleb, D. L. Williamson, and P. J. Rasch, 1996: Description of the NCAR Community Climate Model (CCM3). NCAR Tech. Note NCAR/TN-420+STR, National Center for Atmospheric Research, Boulder, CO, 152 pp.
- King, A. W., W. M. Post, and S. D. Wullschlegel, 1997: The potential response of terrestrial carbon storage to changes in climate and atmospheric CO₂. *Climate Change*, **35**, 199–227.
- Kirschbaum, M. U. F., 2000: Will changes in soil organic carbon act as a positive or negative feedback on global warming? *Biogeochemistry*, **48**, 21–51.
- Koch, G. W., and H. A. Mooney, 1996: Response of terrestrial ecosystems to elevated CO₂: A synthesis and summary. *Carbon Dioxide and Terrestrial Ecosystems*, G. W. Koch and H. A. Mooney, Eds., Academic Press, 415–429.
- Kucharik, C. J., and Coauthors, 2000: Testing the performance of a dynamic global ecosystem model: Water balance, carbon

- balance, and vegetation structure. *Global Biogeochem. Cycles*, **14**, 795–825.
- Landis, J. R., and G. G. Koch, 1977: The measurement of observer agreement for categorical data. *Biometrics*, **33**, 159–174.
- Lloyd, J., and J. A. Taylor, 1994: On the temperature-dependence of soil respiration. *Funct. Ecol.*, **8**, 315–323.
- Maier-Reimer, E., 1993: Biogeochemical cycles in an ocean general-circulation model—Preindustrial tracer distributions. *Global Biogeochem. Cycles*, **7**, 645–677.
- Maltrud, M. E., R. D. Smith, A. J. Semtner, and A. J. Malone, 1998: Global eddy-resolving ocean simulations driven by 1985–1995 atmospheric winds. *J. Geophys. Res.*, **103**, 30 825–30 853.
- Mathews, H. D., A. J. Weaver, and K. J. Meissner, 2005: Terrestrial carbon cycle dynamics under recent and future climate change. *J. Climate*, **18**, 1609–1628.
- McGuire, A. D., and Coauthors, 2001: Carbon balance of the terrestrial biosphere in the twentieth century: Analyses of CO₂, climate and land-use effects with four process-based ecosystem models. *Global Biogeochem. Cycles*, **15**, 183–206.
- Meehl, G. A., W. M. Washington, J. M. Arblaster, and A. Hu, 2004: Factors affecting climate sensitivity in global coupled models. *J. Climate*, **17**, 1584–1596.
- Metz, B., O. Davidson, R. Swart, and J. Pan, Eds., 2001: *Climate Change 2001: Mitigation*. Cambridge University Press, 752 pp.
- Monsrud, R. A., 1990: Methods for comparing global vegetation maps. IIASA Tech. Rep. WP-90-40, International Institute for Applied Systems Analysis, Laxenburg, Austria, 31 pp.
- Mooney, H. A., and Coauthors, 1999: Ecosystem physiology responses to global change. *Implications of Global Change for Natural and Managed Ecosystems. A synthesis of GCTE and Related Research*, B. H. Walker et al., Eds., IGBP Book Series, Vol. 4, Cambridge University Press, 141–189.
- Murphy, J. M., 1995: Transient response of the Hadley Centre coupled ocean–atmosphere model to increasing carbon dioxide. Part III: Analysis of global-mean response using simple models. *J. Climate*, **8**, 496–514.
- Nadelhoffer, K. J., B. A. Emmett, P. Gundersen, O. J. Kjonaas, C. J. Koopmans, P. Schleppi, A. Tietema, and R. F. Wright, 1999: Nitrogen makes a minor contribution to carbon sequestration in temperate forests. *Nature*, **398**, 145–148.
- Najjar, R. G., and J. C. Orr, 1999: Biotic how-to. Revision 1.7, Ocean Carbon-cycle Model Intercomparison Project (OCMIP). [Available online at <http://www.ipsl.jussieu.fr/OCMIP/phase2/simulations/Biotic/HOWTO-Biotic.html>.]
- Nakicenovic, N., and R. Swart, Eds., 2000: *Special Report on Emission Scenarios*. Cambridge University Press, 570 pp.
- Nof, D., 2002: Is there a meridional overturning cell in the Pacific and Indian Oceans? *J. Phys. Oceanogr.*, **32**, 1947–1959.
- Nowak, R. S., D. S. Ellsworth, and S. D. Smith, 2004: Tansley review: Functional responses of plants to elevated atmospheric CO₂—Do photosynthetic and productivity data from FACE experiments support early predictions? *New Phytol.*, **162**, 253–280.
- Orr, R., and Coauthors, 2001: Soil fertility limits carbon sequestration by forest ecosystems in a CO₂-enriched atmosphere. *Nature*, **411**, 469–477.
- Orr, J. C., and J.-C. Dutay, 1999: OCMIP mid-project workshop. *Research GAIM Newsletter*, Vol. 3, No. 1, 4–5.
- , and Coauthors, 2001: Estimates of anthropogenic carbon uptake from four 3-D global ocean models. *Global Biogeochem. Cycles*, **15**, 43–60.
- Owensby, C. E., J. M. Ham, A. K. Knapp, and L. M. Auen, 1999: Biomass production and species composition change in a tall grass prairie ecosystem after long-term exposure to elevated atmospheric CO₂. *Global Change Biol.*, **5**, 497–506.
- Prentice, I. C., M. Heimann, and S. Sitch, 2000: The carbon balance of the terrestrial biosphere; ecosystem models and atmospheric observations. *Ecol. Appl.*, **10**, 1553–1573.
- , and Coauthors, 2001: The carbon cycle and atmospheric carbon dioxide. *Climate Change 2001: The Scientific Basis*, J. T. Houghton et al., Eds., Cambridge University Press, 183–237.
- Ramankutty, N., and J. A. Foley, 1999: Estimating historical changes in global land cover: Croplands from 1700 to 1992. *Global Biogeochem. Cycles*, **13**, 997–1027.
- , —, J. Norman, and K. McSweeney, 2002: The global distribution of cultivable lands: Current patterns and sensitivity to possible climate change. *Global Ecol. Biogeogr.*, **11**, 377–392.
- Root, T. L., and S. H. Schneider, 1993: Can large-scale climatic models be linked with multiscale ecological studies? *Conserv. Biol.*, **7** (2), 256–270.
- Sabine, C. L., and Coauthors, 2004: The oceanic sink for anthropogenic CO₂. *Science*, **305**, 367–371.
- Sarmiento, J. L., and C. Le Quere, 1996: Oceanic carbon dioxide uptake in a model of century-scale global warming. *Science*, **274**, 1346–1350.
- , T. C. Hughes, R. J. Stouffer, and S. Manabe, 1998: Simulated response of the ocean carbon cycle to anthropogenic climate warming. *Nature*, **393**, 245–249.
- Schimel, D. S., 1998: The carbon equation. *Nature*, **393**, 208–209.
- Senior, C. A., and J. F. B. Mitchell, 2000: The time dependence of climate sensitivity. *Geophys. Res. Lett.*, **27**, 2685–2688.
- Shaw, M. R., E. S. Zavaleta, N. R. Chiariello, E. E. Cleland, H. A. Mooney, and C. B. Field, 2002: Grassland responses to global environmental changes suppressed by elevated CO₂. *Science*, **298**, 1987–1990.
- Thompson, S., B. Govindasamy, A. Mirin, K. Caldeira, C. Delire, J. Milovich, M. Wickett, and D. Erickson, 2004: Quantifying the effects of CO₂-fertilized vegetation on future global climate and carbon dynamics. *Geophys. Res. Lett.*, **31**, L23211, doi:10.1029/2004GL021239.
- Tjoelker, M. G., J. Oleksyn, and P. B. Reich, 2001: Modelling respiration of vegetation: Evidence for a general temperature-dependent Q(10). *Global Change Biol.*, **7**, 223–230.
- Washington, W. M., and Coauthors, 2000: Parallel Climate Model (PCM) control and transient simulations. *Climate Dyn.*, **16**, 755–774.
- Zeng, N., H. Qian, E. Munoz, and R. Iacono, 2004: How strong is carbon cycle-climate feedback under global warming? *Geophys. Res. Lett.*, **31**, L20203, doi:10.1029/2004GL020904.